Mansoura Engineering Journal

Volume 28 | Issue 2 Article 14

1-20-2021

Numerical and Experimental Studies on Plastic Solar Air Heaters for Heating Processes.

M. Bassiouny
Mechanical Power Engineering Department., Minufiya University., Faculty of Engineering., Shebin El-Kom, Egypt

NUMERICAL AND EXPERIMENTAL STUDIES ON PLASTIC SOLAR AIR-HEATERS FOR HEATING PROCESSES

دراسات عددية ومعملية على مسخنات هواء شمسية من البلاستيك لعمليات التسخين

M. Khalil Bassiouny
Minufiya University, Faculty of Engineering, Mechanical Power Department, Shebin El-Kom, Egypt
E-mail mkhalilb@hotmail.com

الخلاصة:

تم تقديم دراسة نظرية تشتمل على تحليل انتقال الحرارة بالحمل والإشعاع المشترك لمسخن هواء شمسي من النوع الأسطواني المرن المستخدم في عمليات التسخين. يصنع المجمع الشمسي من طبقتين من البلاستيك تعملان كمصاص أسود وغطاء نفاذ للأشعة الشمسية وملتصقتين معا على طول حفتيهما. ينفخ المجمع الشمسي بواسطة الهواء المضغوط المتدفق.

تم كتابة برنامج على الحاسب الآلي لحساب الكفاءة الحرارية وكفاءة الطاقة المستفادة للمجمع الشمسي. كما تم تطبيق طريقة التكامل الخطي لحساب الإشعاع المتبادل بين المصاص والغطاء اللازم لتقييم أداء المجمع الشمسي. يعطي هذا التحليل معادلات لحساب معامل الشكل في حالة مجمعات شمسية محملة جزئيا وكليا ذات أطوال ونسب بعدية مختلفة. تم أيضا إجراء تجارب عملية خارج المعمل على ثلاثة أنواع من مسخنات الهواء الشمسية الأسطوانية المرنة ذات غطاء مفرد وكذلك ذات غطاء مزدوج ومجهزة بعازل خلفي أو بدونه. أظهرت الاختبارات أن مسخن الهواء الشمسي ذو الغطاء المزدوج والعازل الخلفي يحظى بكفاءة أعلى من مثيله ذو الغطاء المفرد وبدون عازل خلفي. كذلك تم تعيين رقم نوسلت بين المصاص والهواء المسخن بدلالة رقم رينولدز عمليا.

تشير المقارنات بين البيانات العملية والطريقة العددية لكفاءة المجمع الشمسي إلى اتفاق جيد. تم أيضا استنباط معادلة تجريبية لرقم نوسلت ومقارنتها مع معادلة تجريبية لمؤلفين آخرين.

ABSTRACT

A theoretical study including the combined convective and radiative heat transfer analysis of a flexible cylindrical type solar air-heater for heating processes is presented. The solar collector is manufactured from PVC films acting as a black absorber and a transparent cover sealed together along its edges. The collector is to be blown with a flow of pressurized air.

A computer program is written for calculating the collector thermal and exergy efficiencies. The contour (line) integral method is applied for predicting the diffuse radiation interchange between the absorber and the cover. The analysis yields expressions for calculating the configuration factor in case of part-loaded and full-loaded collectors for different lengths and aspect ratios. Outdoors experimental investigations are carried out on three types of flexible

Accepted June 30, 2003.

cylindrical solar air-heaters with a single cover as well as double covers with and without a back insulation. The tests show that the solar air-heater having double covers and a back insulation has the highest efficiency,while that of a single cover and without a back insulation has the lowest efficiency. Moreover, the Nusselt number between the absorber and the heated air is determined experimentally in relation with the Reynolds number.

Comparisons between the experimental data and the theoretical methods for the collector efficiency and the configuration factor demonstrate a good agreement. In addition of this, the present experimental results of Nusselt number are correlated and compared with a correlation of another authors.

Keywords: ***Solar collectors, air-heaters, theoretical analysis, experimental investigations, performance, and configuration factor.***

NOMENCLATURE

A	area, m^2
a	half major axis of part loaded collector (elliptic cylinder), m
b	half minor axis of part loaded collector (elliptic cylinder), m
C	constant
C_1	contour of area A_1, m
C_2	contour of area A_2, m
c_p	specific heat at constant pressure, J/kg K
D	diameter of collector, m
D_n	day number
E	exergy, W
F	radiation configuration factor
h	heat transfer coefficient, W/m^2K
h_s	solar hour angle, °
I	total enthalpy, W
I_c	solar insolation, W/m^2
I_o	solar constant, (I_o = 1353 W/m^2)
i	specific enthalpy, J/kg
k	thermal conductivity of air, W/mK
L	length of collector, m
L^*	site latitude, °
m	air mass, kg
$\dot{m}$	mass flow rate of air in collector, kg/s
NTU	Number of Transfer Units
P	perimeter, m
p	pressure, Pa
$\dot{Q}$	rate of heat transfer, W
$\dot{q}$	heat flux, W/m^2

R radius of full loaded collector, m
r distance between two arbitrary points one on the absorber and the other on the cover, m
S entropy, W/K
x, y, z cartesian coordinates
Z altitude, m

Greek symbols

α absorptivity
α_s solar altitude angle, °
β_1 angle between the normal to area element dA_1 and the connecting line between dA_1 and dA_2, °
β_2 angle between the normal to area element dA_2 and the connecting line between dA_1 and dA_2, °
δ expression defined by eq.(36)
δ_s declination angle of sun, °
Δ difference
ε emissivity
η efficiency
λ aspect ratio in case of part-loaded collector, $(\lambda = b/a)$
ρ density, kg/m^3
σ Stefan - Boltzmann constant, ($\sigma = 5.6687 \times 10^{-8}$ W/m^{2}K^4)
τ transmissivity
τ_{atm} atmospheric transmittance
φ cylindrical coordinate
ψ ratio between radius and length in case of full-loaded collector, $(\psi = R/L)$
Ω expression defined by eq.(35)
ω ratio between half major axis and length in case of part-loaded collector, $(\omega = a/L)$

Subscripts

a absorber
bl back loss
c cover
con convection
e exergy
f fluid
in inlet
m mean
out outlet
p projected

r	radiation
s	solar
t	thermal
u	useful
∞	ambient

INTRODUCTION

Solar energy is the world's most abundant permanent source of energy. The amount of solar energy intercepted by the planet earth is 170 trillion kW, an amount 5,000 times greater than the sum of all other inputs (terrestrial, nuclear, geothermal, and gravitational energies and lunar gravitational energy). Of this amount 30% is reflected to space, 47% is converted to low-temperature heat and re-radiated to space, 23% powers the evaporation / precipitation cycle of the biosphere, less than ½% represents the kinetic energy of the wind, waves and in photosynthetic storage in plants.

Solar energy is transmitted from the sun through space to earth by electromagnetic radiation. It must be converted to heat before it can be used in practical heating or cooling systems. Solar energy collectors are the devices used to convert the sun's radiation to heat. They consist of a surface that efficiently absorbs radiation and converts it to heat, which raises the temperature of the absorbing material. A part of this energy is then removed from the absorbing surface by means of a heat transfer fluid that may be either water or air.

The heating of air using solar energy has been the subject of many articles [1-4]. Flat plate solar collectors are perhaps the common devices for interception solar heat at low temperatures, and had been used extensively for heating purposes. In the past few years, a considerable number of papers had been published relating to the actual design, optimization of parameters and performance of solar-air heaters [5-11]. Most of the work reported in the literature requires a considerable amount of effort for performance prediction of new designs of solar-air heaters. Since the numbers of variables are large, it becomes a tedious job to predict the efficiency of a new heater design.

The using of plastic cylindrical type solar energy collectors for heating air is regarded as a practical method for crops dehydration and heating processes. This type of collectors can be manufactured as a cylinder (after blowing) with the upper half of a transparent flexible plastic material and the lower half of a black one. It can be made of different lengths and diameters or aspect ratios with one or two covers and also with back insulation. The collector is to be blown with pressurized air.

The analysis of radiation interchange among diffusely emitting and reflecting surfaces depends mainly on the configuration (angle) factor, see [12-15], which is a dimensionless quantity representing the fraction of the radiant energy leaving one surface and arrives at a second surface. When the radiant energy leaving a surface is diffusely distributed according to Lambert's Cosine Law [16], the following mathematical relations apply:

$$F_{A_1-A_2} = \frac{1}{A_1} \oint_{A_1} \oint_{A_2} \frac{\cos\beta_1 . \cos\beta_2}{\pi r^2} dA_1\, dA_2 \qquad \ldots (1)$$

And

$$A_1 F_{A_1-A_2} = A_2 F_{A_2-A_1} . \qquad \ldots (2)$$

In practice, the integration, given by eq.(1) may be quite difficult even for simple geometry. It is not possible to complete the analytical integration and obtain closed-form representation of the angle factor. A new representation for angle factor had been derived by Sparrow [17], which replaces the usual area integral by more tractable contour integral. The new formulation generally simplifies analytical calculation of angle factor. The advantages of this representation are associated with the reduced order of the integrals (the former double integral is reduced to a single one and the former quadruple integral is reduced to a double one). The basic tool needed in carrying out the transformation is Stokes' theorem [18].

The study presented here is theoretical and experimental investigations for combined radiative and convective heat transfer in flexible cylindrical type solar-air heaters. The aim of this work is to determine the performance of the solar collector considered. From another hand, since the radiation configuration factor is necessary for predicting the performance of solar collectors and there are no informations yet about this factor, in case of the cylindrical collector type, the objective of the present work is to derive mathematical expression for calculating the configuration factor. The analysis covers both cases of part – loaded and full - loaded collectors.

PERFORMANCE OF THE SOLAR COLLECTOR

Energy balance of the absorber

In case of the steady-state conditions, the energy balance of absorber of the solar air-heater considered, Fig.1, can be formulated by the following relation:

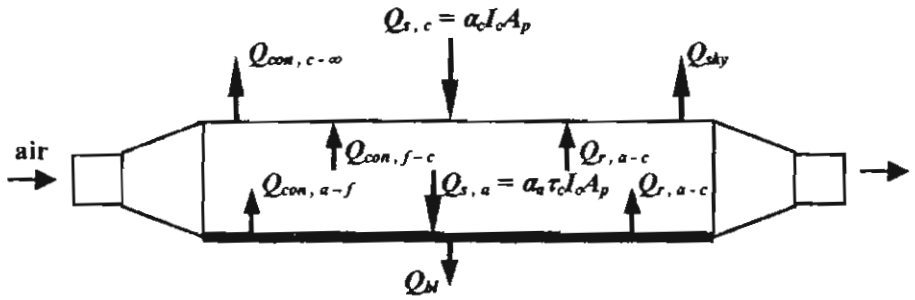

Fig. 1: Energy balance of both absorber and cover

$$\dot{Q}_{s,a} = \dot{Q}_{con,a-f} + \dot{Q}_{r,a-c} + \dot{Q}_{bl} \qquad \ldots (3)$$

where,

$$\dot{Q}_{s,a} = \alpha_a \tau_c I_c A_p, \quad \ldots (4)$$

$$\dot{Q}_{con,a-f} = h_{con,a-f} A\left(T_a - T_{f,m}\right), \quad \ldots (5)$$

$$\dot{Q}_{r,a-c} = \frac{\sigma A}{\frac{1}{\varepsilon_a} + \frac{1}{\varepsilon_c} + \frac{1}{F_{a-c}} - 2}\left(T_a^4 - T_c^4\right), \quad \ldots (6)$$

$$\dot{Q}_{bl} = h_{con,a-\infty} A\left(T_a - T_\infty\right). \quad \ldots (7)$$

Inserting eqs.(4 - 7) into eq.(3), results in

$$\alpha_a \tau_c I_c \frac{A_p}{A} = h_{con,a-f}\left(T_a - T_{f,m}\right) + \frac{\sigma}{\frac{1}{\varepsilon_a} + \frac{1}{\varepsilon_c} + \frac{1}{F_{a-c}} - 2}\left(T_a^4 - T_c^4\right) + h_{con,a-\infty}\left(T_a - T_\infty\right). \quad \ldots (8)$$

Energy balance of the cover

The energy balance of the cover can be represented, according to Fig.1, by the following expression

$$\dot{Q}_{s,c} + \dot{Q}_{con,f-c} + \dot{Q}_{r,a-c} = \dot{Q}_{con,c-\infty} + \dot{Q}_{sky}. \quad \ldots (9)$$

where,

$$\dot{Q}_{s,c} = \alpha_c I_c A_p, \quad \ldots (10)$$

$$\dot{Q}_{con,f-c} = h_{con,f-c} A\left(T_{f,m} - T_c\right), \quad \ldots (11)$$

$$\dot{Q}_{con,c-\infty} = h_{con,c-\infty} A\left(T_c - T_\infty\right), \quad \ldots (12)$$

$$\dot{Q}_{sky} = \varepsilon_c \sigma A\left(T_c^4 - T_{sky}^4\right). \quad \ldots (13)$$

Substituting eq.(6) and eqs.(10-13) into eq.(9), the following relation yields

$$\alpha_c I_c \frac{A_p}{A} + h_{con,f-c}\left(T_{f,m} - T_c\right) + \frac{\sigma}{\frac{1}{\varepsilon_a} + \frac{1}{\varepsilon_c} + \frac{1}{F_{a-c}} - 2}\left(T_a^4 - T_c^4\right) = h_{con,c-\infty}\left(T_c - T_\infty\right) + \varepsilon_c \sigma\left(T_c^4 - T_{sky}^4\right). \quad \ldots (14)$$

Energy balance of a fluid element

An energy balance of the fluid element, sketched in Fig.2, gives the following equation:

$$\dot{m} i + \dot{q}_{con,a-f}\,\Delta A = \dot{m}\left(i + \Delta i\right) + \dot{q}_{con,f-c}\,\Delta A. \quad \ldots (15)$$

Substituting eq.(5) into eq.(15) and applying Taylor series gives

$$\dot{m}i + h_{con,a-f}\left(\tfrac{1}{2}P\Delta X\right)\left(T_a - T_f(X)\right) = \dot{m}\left(i + \frac{di}{dX}\Delta X\right) + h_{con,f-c}\left(\tfrac{1}{2}P\Delta X\right)\left(T_f(X) - T_c\right)$$

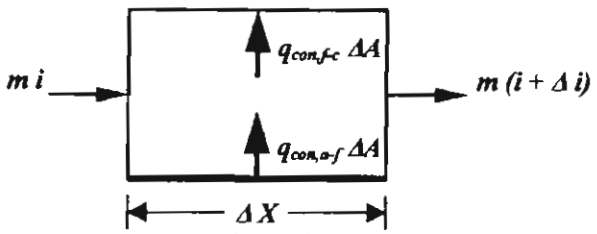

Fig. 2: Energy balance of a fluid element

One obtains, after collecting the terms and putting $i = c_p T_f(X)$,

$$\frac{\dot{m}c_p}{\frac{1}{2}P}\frac{dT_f(X)}{dX} = h_{con,a-f}\left(T_a - T_f(X)\right) - h_{con,f-c}\left(T_f(X) - T_c\right).$$

Taking into account that $h_{con,a-f} = h_{con,f-c}$,

$$\therefore \frac{\dot{m}c_p}{\frac{1}{2}P}\frac{dT_f(X)}{dX} = h_{con,a-f}\left(T_a + T_c - 2T_f(X)\right).$$

Let $NTU = \dfrac{h_{con,a-f}A}{\dot{m}c_p} = \dfrac{h_{con,a-f}\left(\frac{1}{2}PL\right)}{\dot{m}c_p}$ and $x = \dfrac{X}{L}$, we have

$$\frac{dT_f(x)}{dx} = NTU\left(T_a + T_c - 2T_f(x)\right). \quad \ldots (16)$$

The integration of eq.(16) results in

$$T_f(x) = \tfrac{1}{2}\left[\left(T_a + T_c\right) - C\,e^{-2NTU\,x}\right]. \quad \ldots (17)$$

The boundary conditions associated with eq.(17) are

at $x = 0$, $T_f = T_{in}$ and at $x = 1$, $T_f = T_{out}$.

The substitution of the preceding boundary conditions in eq.(17) gives

$$T_{out} = \tfrac{1}{2}\left[\left(T_a + T_c\right) - \left(T_a + T_c - 2T_{in}\right)e^{-2NTU}\right]. \quad \ldots (18)$$

Collector thermal efficiency

The collector thermal efficiency may be defined and calculated from the following relation

$$\eta_t = \frac{\textit{useful energy delivered}}{\textit{total incoming solar energy}} = \frac{\dot{Q}_u}{A_p I_c} = \frac{2\dot{Q}_u}{\pi DLI_c}. \quad \ldots (19)$$

The useful energy delivered is the energy carried away by the flowing air, which is equal to

$$\dot{Q}_u = \dot{m} c_p (T_{out} - T_{in}). \quad \ldots (20)$$

The substitution of eq.(20) into eq.(19), making use of eq.(18), yields

$$\eta_t = \frac{2\dot{m} c_p (T_{out} - T_{in})}{\pi DLI_c} = \frac{\dot{m} c_p (T_a + T_c - 2T_{in})\left(1 - e^{-2NTU}\right)}{\pi DLI_c} \quad \ldots (21)$$

Collector exergy efficiency

The exergy gain ΔE by the collector, which means the maximum available work obtained from the thermal energy gain is given by

$$\Delta E = \Delta I - T_\infty \Delta S \quad \ldots (22)$$

where, ΔE is the *exergy* gain and ΔI refers to the *enthalpy* gain while, $T_\infty \Delta S$ represents the *anergy* where,

$$\Delta I = \dot{Q}_u = \dot{m} c_p (T_{out} - T_{in}), \text{ and}$$

$$\Delta S = \dot{m} c_p \ln\left(\frac{T_{out}}{T_{in}}\right).$$

Therefore, the exergy gain becomes

$$\Delta E = \dot{m} c_p \left[T_{out} - T_{in} - T_\infty \ln\left(\frac{T_{out}}{T_{in}}\right)\right]. \quad \ldots (23)$$

The exergy efficiency, η_e, is expressed as follows

$$\eta_e = \frac{\textit{maximum available work}}{\textit{total incoming solar energy}} = \frac{\Delta E}{A_p I_c}$$

$$= \frac{2\dot{m} c_p \left[T_{out} - T_{in} - T_\infty \ln(T_{out}/T_{in})\right]}{\pi DLI_c}. \quad \ldots (24)$$

NUMERICAL SOLUTION

Equations (8), (14) and (18) are three simultaneous quartic algebraic equations in the three unknowns cover, absorber and air outlet temperatures. These equations can be solved numerically using the *Newton-Raphson* iterative procedure [19]. For this purpose, a computer program is written and developed for solving the above mentioned three equations and determining the collector thermal efficiency as well as the exergy efficiency. The solutions are obtained in terms of the influencing parameters such as the collector diameter, the collector length, air mass flow rate, air inlet temperature, and the solar insolation.

ANALYTICAL STUDY

Radiation configuration factor

The area integral appearing in eq.(1) usually implies a quadruple integration. A reduction in the multiplicity of the integration can be achieved by employing contour integrals instead of area integral. The reduction in multiplicity is especially advantageous when numerical evaluation is required. The contour integral representation is as follows:

$$F_{A_1-A_2} = \frac{1}{2\pi A_1} \int_{C_2} \int_{C_1} \left(\ln r . dx_1 dx_2 + \ln r . dy_1 dy_2 + \ln r . dz_1 dz_2 \right). \quad \ldots (25)$$

In eq.(25), the integrations are performed around the contours C_1 and C_2 that respectively bound the areas A_1 and A_2. The coordinates (x_1, y_1, z_1) and (x_2, y_2, z_2) correspond to points on the respective boundaries, and r is the distance between such boundary points, as shown in Fig.3.

Part-loaded collector

At no load, which is corresponding to the case of no air flow, both the cover and absorber of the solar air-heater will lie on each other. Therefore, the configuration factor should be equal to unity. When the solar collector is set in operation by circulating pressurized air, the configuration factor is expected to be less than unity. At part-loaded collector, which is corresponding to the case when the air flow rate is lower than the maximum designed value, the collector will take the form of an elliptical cylinder. Figure 3 represents a schematic diagram of the solar air-heater considered and coordinates for computation of the configuration factor.

In terms of rectangular coordinates system, the distance r between any point $P(x_1, y_1, z_1)$ on the absorber surface and any point $Q(x_2, y_2, z_2)$ on the cover surface can be calculated as

$$r = \sqrt{(x_1 - x_2)^2 + (y_1 - y_2)^2 + (z_1 - z_2)^2}. \quad \ldots (26)$$

In cylindrical coordinates system

$$x = a\cos\phi, \quad \ldots (27)$$

and

$$y = b\sin\phi. \quad \ldots (28)$$

Substituting eqs.(27) and eq.(28) in eq.(26) and collecting the terms, one obtains

$$r = \sqrt{(a^2 - b^2)\left[\cos^2\phi_1 + \cos^2\phi_2 - \cos(\phi_1 + \phi_2)\right] - (a^2 + b^2)\cos(\phi_1 - \phi_2) + 2b^2 + (z_1 - z_2)^2} \quad \ldots (29).$$

Differentiating eqs.(27) and (28) and substituting in eq.(25) yields:

$$2\pi A_1 F_{A_1-A_2} = \int_{C_2} \int_{C_1} \ln r . \left(a^2 \sin\phi_1 \sin\phi_2\right) d\phi_1 d\phi_2 + \int_{C_2} \int_{C_1} \ln r . \left(b^2 \cos\phi_1 \cos\phi_2\right) d\phi_1 d\phi_2$$

$$+ \int_{C_1} \int_{C_1} \ln r . dz_1 dz_2 . \quad \ldots (30)$$

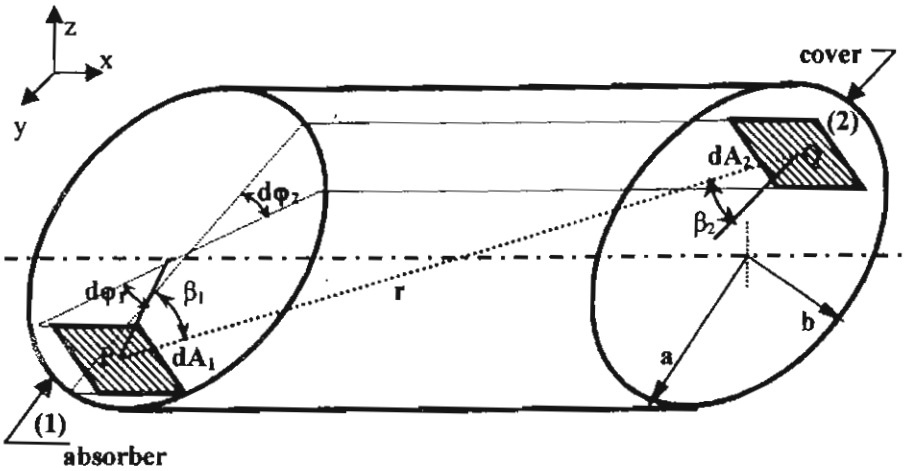

Fig. 3: Plastic solar air-heater with nomenclature and coordinates x,y,z for computation of the configuration factor

The foregoing equation represents the contour integral of the configuration factor for radiant interchange between the absorber and cover of the solar air-heater under part load condition. In performing the integration, it may be noted that on all segments of C_1 either $d\phi_1 = 0$ or $dz_1 = 0$. Also, either $d\phi_2 = 0$ or $dz_2 = 0$ on all segments of C_2. Therefore, eq.(30) may be reduced to

$$2\pi A_1 F_{A_1-A_2} = \int_{C_2}\int_{C_1} \ln r.dz_1 dz_2 . \qquad \ldots (31)$$

The substitution of eq.(29) into eq.(31) gives

$$2\pi A_1 F_{A_1-A_2} = \frac{1}{2}\int_{C_2}\int_{C_1} \ln \left\{ \begin{matrix} \left(a^2-b^2\right)\left[\cos^2\phi_1+\cos^2\phi_2-\cos(\phi_1+\phi_2)\right]- \\ \left(a^2+b^2\right).\cos(\phi_1-\phi_2)+2b^2+(z_1-z_2)^2 \end{matrix} \right\} dz_1 dz_2 . \qquad \ldots (32)$$

The first step is to specialize the contour integral around C_1, where $\phi_1 = 0$ and $\phi_2 = \pi$, this results in

$$2\pi A_1 F_{A_1-A_2} = \frac{1}{2}\int_{C_2} dz_2 \int_0^L \ln \left\{ \begin{matrix} \left(a^2-b^2\right)\left(1+\cos^2\phi_2-\cos\phi_2\right)- \\ \left(a^2+b^2\right).\cos\phi_2+2b^2+(z_1-z_2)^2 \end{matrix} \right\} dz_1 +$$

$$\frac{1}{2}\int_{C_2} dz_2 \int_L^0 \ln \left\{ \begin{matrix} \left(a^2-b^2\right)\left[1+\cos^2\phi_2-\cos(\pi+\phi_2)\right]- \\ \left(a^2+b^2\right).\cos(\pi-\phi_2)+2b^2+(z_1-z_2)^2 \end{matrix} \right\} dz_1 .$$

The next step is to evaluate the contour integral around C_2, where $\phi_1 = 2\pi$ and $\phi_2 = \pi$

$$2\pi A_1 F_{A_1-A_2} = \frac{1}{2}\int_0^L\int_0^L \ln\left[\left(a^2-b^2\right)-\left(a^2+b^2\right)+2b^2+(z_1-z_2)^2\right] dz_1 dz_2$$

$$+\frac{1}{2}\int_{L}^{0}\int_{0}^{L}\ln\left[3\left(a^2-b^2\right)+\left(a^2+b^2\right)+2b^2+\left(z_1-z_2\right)^2\right]dz_1dz_2$$

$$+\frac{1}{2}\int_{0}^{L}\int_{L}^{0}\ln\left[3\left(a^2-b^2\right)+\left(a^2+b^2\right)+2b^2+\left(z_1-z_2\right)^2\right]dz_1dz_2$$

$$+\frac{1}{2}\int_{L}^{0}\int_{L}^{0}\ln\left[\left(a^2-b^2\right)+\left(a^2+b^2\right)+2b^2+\left(z_1-z_2\right)^2\right]dz_1dz_2 .$$

Collecting the terms, the foregoing equation becomes

$$2\pi A_1 F_{A_1-A_2}=2\int_{0}^{L}\int_{0}^{L}\ln\left(z_1-z_2\right)dz_1dz_2+\int_{0}^{L}\int_{L}^{0}\ln\left[4a^2+\left(z_1-z_2\right)^2 dz_1dz_2\right]. \quad \ldots (33)$$

The surface area of the absorber A_1 (half-elliptic cylinder surface) is equal to

$$A_1=\frac{\pi}{2}(a+b)L\,\Omega \ . \quad \ldots (34)$$

where

$$\Omega=1+\frac{1}{4}\delta^2+\frac{1}{64}\delta^4+\frac{1}{256}\delta^6+\frac{25}{16384}\delta^8+\ldots\ldots, \quad \ldots (35)$$

with

$$\delta=\frac{a-b}{a+b}=\frac{1-\lambda}{1+\lambda} \quad \ldots (36)$$

and λ is the aspect ratio, $\lambda=b/a$.

When λ goes to 0, Ω approaches $4/\pi$ and when λ goes to unity, Ω approaches unity also. The required double integrals in eq.(33) can be carried out with the aid of standard tables of integration [20]. The final expression for the configuration factor for radiation heat exchange between the cover and absorber of the solar air-heater considered at part-loaded collector can be stated in the following form:

$$F_{a-c}=\frac{2}{\pi^2(1+\lambda)\Omega}\left[4\omega\ln(2\omega)+\frac{1-4\omega^2}{2\omega}\ln\left(1+4\omega^2\right)+4\tan^{-1}\frac{1}{2\omega}\right] \quad \ldots (37)$$

The previous equation holds for $\lambda)0$, where, $\omega=a/L$.

Full-loaded collector

When the solar collector is operating under full load condition, i.e. with maximum designed air flow rate, it takes a circular cylinder shape. It may be considered as a limit case of the part load condition with $\lambda=1$ and consequently $\Omega=1$. Therefore, the configuration factor represented by eq.(37) may be reduced in case of full load to

$$F_{a-c}=\frac{1}{\pi^2}\left[4\psi\ln(2\psi)+\frac{1-4\psi^2}{2\psi}\ln\left(1+4\psi^2\right)+4\tan^{-1}\frac{1}{2\psi}\right]. \quad \ldots (38)$$

where, $\psi=R/L$.

Case of infinite length

When the solar collector is so long that there is no more energy dissipation by radiation from the open ends, i.e. L approaches ∞ or ω goes to zero, the configuration factor can easily and directly be determined from Fig. 4 using the reciprocity theorem [15] as follows:

$A_1 F_{A_1-A_3} = A_3 F_{A_3-A_1} = A_3 \times 1$, and

$F_{A_1-A_3} = F_{A_1-A_2}$.

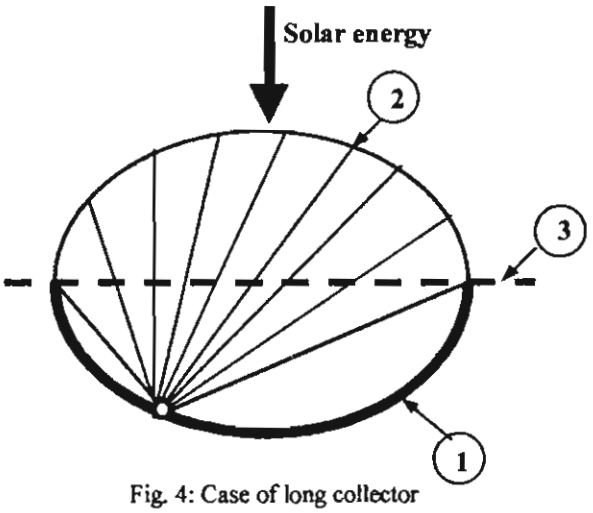

Fig. 4: Case of long collector

Therefore

$$F_{a-c} = \frac{A_3}{A_1} = \frac{2aL}{\pi(a+b)L\,\Omega/2} = \frac{4}{\pi(1+\lambda)\Omega}. \qquad \ldots (39)$$

It can be seen from eq.(39) that with no air flow ($b = 0, \lambda = 0, \Omega = 4/\pi$), $F_{a-c} = 1$ and at full-loaded collector ($b = a = R, \lambda = 1, \Omega = 1$) & $F_{a-c} = 2/\pi$.

ESTIMATION OF SOLAR INSOLATION

The total solar energy reaching the earth is made up of two parts: the energy in the direct beam and the diffuse energy from the sky. Most manmade solar collectors can convert only direct energy efficiently. The amount of direct energy depends on the cloudiness and the position of the sun and is obviously greatest on clear days. The following calculation procedure is applied for estimating the solar insolation [6].

The site latitude, L^*, of Shebin El Kom, Egypt is predicted from the atlas to be

$L^* = +31.25^o$. ... (40)

The positive sign means north of the equator. The solar hour angle, h_s, is equal to 15° times the number of hours from local solar noon, i.e.

$h_s = 15^o \times (12 - hour)$. ... (41)

The declination angle of the sun, δ_s, is the angle between the sun's rays and the zenith direction at noon on the earth's equator, i.e.

$$\delta_s = 23.44 \times \sin\left[\frac{360}{365}(284 + D_n)\right], \quad \ldots (42)$$

where, D_n is the day number from the first of January.

In order to calculate the solar-altitude angle α_s, the following relation can be applied [6]

$$\sin\alpha_s = \sin L^{\bullet} \times \sin\delta_s + \cos L^{\bullet} \times \cos\delta_s \times \cos h_s . \quad \ldots (43)$$

The air mass, $m(0,\alpha_s)$, at sea level (altitude Z = 0) is given by

$$m(0,\alpha_s) = \left[1229 + (614 \times \sin\alpha_s)^2\right]^{\frac{1}{2}} - 614 \times \sin\alpha_s . \quad \ldots (44)$$

The atmospheric transmittance, τ_{atm}, at sea level (Z = 0) is given, to within 3% accuracy for clear skies, by the following equation [6]

$$\tau_{atm} = \frac{I_c}{I_o} = 0.5\left[e^{-0.65\,m(0,\alpha_s)} + e^{-0.095\,m(0,\alpha_s)}\right],$$

where, $I_o = 1353$ W/m^2 = the solar constant.

The solar insolation, I_c, can be now estimated from the following relation

$$I_c = 0.5\,I_o\left[e^{-0.65\,m(0,\alpha_s)} + e^{-0.095\,m(0,\alpha_s)}\right]. \quad \ldots (45)$$

A Fortran computer program is written for estimating the daily and seasonal variations of solar insolation in Shebin El Kom, Egypt using eqs.(40) to (45).

EXPERIMENTAL INVESTIGATIONS

In order to test the performance of a plastic cylindrical-type solar air-heater with different design parameters and under variable operating conditions, an experimental setup is constructed, as shown in Fig. 5, in the solar energy laboratory, Minufiya University, Faculty of Engineering. The air-heater, in its simplest design, consists of a plastic hose with 0.57 m diameter and 20 m length. It is made of a black PVC sheet of 0.7 mm thickness acting as an absorber and a transparent cover of PVC having 0.6 mm thickness. Both sheets are sealed together along their edges. Holes are made in the edges and ropes are used for the sake of fixation, as represented by the white lines in Fig. 5.

The collector is blown with a flow of pressurized air using an air blower having a maximum discharge of about 1400 m^3/h. The air flow rate is controlled by means of a throttle valve to the desired value. An orifice meter is calibrated with the help of a bellows meter of 0.05 m^3 resolution (for measuring the volume of air) and a stop watch in order to determine the air flow rate by measuring the pressure drop across it using a water U-tube manometer. A Bourdon's tube pressure gauge of 0.1 bar resolution is used for measuring the air pressure at inlet while a mercury glass thermometer of 0.2°C resolution is used for measuring the ambient temperature in order to predict the air density.

Air temperature measurements are carried out with copper-constantan thermocouple probes of about 1 mm bead diameter. A thermocouple probe

located at the center of the inlet section measures the inlet air temperature. The hot air is mixed in a mixing chamber after leaving the solar collector in order to measure the outlet bulk temperature of air using a single thermocouple probe. The cover and absorber temperatures are measured along the solar collector by means of five thermocouple probes clapped on each surface at equal distances. The average temperature of each surface is obtained as the arithmetic mean of the five-thermocouple readings. The readings are observed periodically to check time dependent measurements. After reaching the steady- state condition, all the measured variables are recorded.

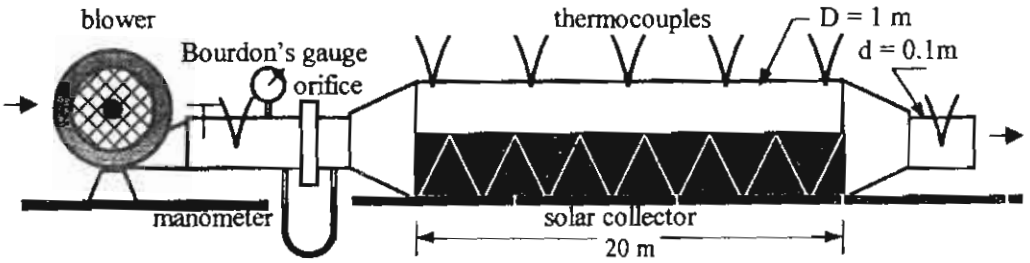

Fig. 5: Experimental setup

Outdoors experimental investigations are carried out under clear skies on three types of flexible cylindrical solar air-heaters with a single cover as well as double covers with and without a back insulation. In case of solar air-heaters with back insulation, about 5 cm layer of sawdust is held between the back side of the absorber and a PVC casing sheet to minimize the energy loss through the bottom. In order to compare their performance, the standard test method of the National Bureau of Standards (NBS), Ref.[21], is performed using the instantaneous test procedure.

Nusselt number

The convective heat transfer film coefficient between the absorber and the flowing air can be calculated from the following relation:

$$h_{con,a-f} = \frac{\dot{Q}_u}{A(T_a - T_{f,m})} = \frac{\dot{m} c_p (T_{out} - T_{in})}{A(T_a - T_{f,m})}$$

where $T_{f,m}$ is the air mean temperature, which is given by

$$T_{f,m} = \frac{T_{in} + T_{out}}{2}.$$

The Nusselt number is defined as

$$Nu = \frac{h_{con,a-f} D}{k}$$

RESULTS AND DISCUSSION

Figure 6 indicates the theoretical results obtained for the collector thermal efficiency against the appropriate parameter $\Delta T/I_c$ for a fixed value of the collector length ($L = 20$ m) and different values of the collector diameter. The figure shows that the collector thermal efficiency decreases linearly with the parameter $\Delta T/I_c$ and it decreases also with increasing the collector diameter. The former is because the configuration factor between the absorber and the cover becomes lower with increasing the collector diameter. The effect of the collector length on the thermal efficiency is presented in Fig.7 and Fig.8 for $D = 0.5$ m and 2 m respectively. It is clear from the figure that the thermal efficiency increases as the collector length increases. This is also due to the increase of the configuration factor with the collector length. The rate of increase is high for short lengths of collector and it becomes relatively insignificant for long collectors (longer as 30 m).

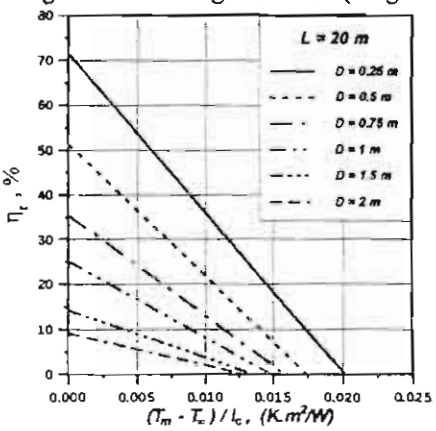

Fig. 6: Thermal efficiency as a function of the collector diameter, L = 20 m

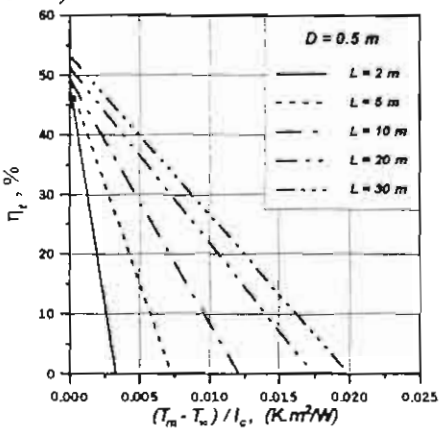

Fig. 7: Thermal efficiency as a function of the collector length, D = 0.5 m

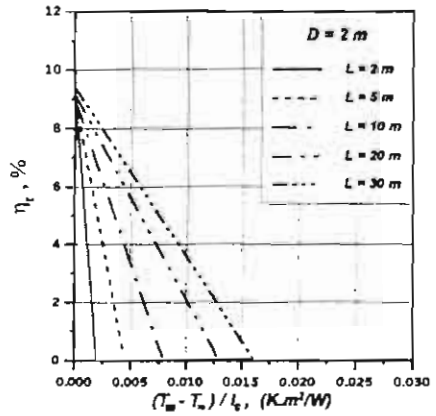

Fig. 8: Thermal efficiency as a function of the collector length, D = 2 m

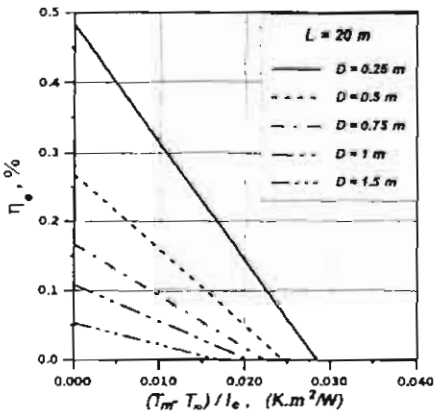

Fig. 9: Exergy efficiency as a function of the collector diameter

From the standpoint of exergy, Fig.9 represents the variation of the collector exergy efficiency with the collector diameter while Fig.10 represents the same variation but with the collector length. It is seen that the exergy efficiency of the collector decreases with increasing its diameter while it increases with increasing its length. The exergy efficiency has much lower values than the thermal efficiency.

Figure 11 shows the variation of the configuration factor between the absorber and cover of the plastic type solar air-heater at part-loaded collector (case of elliptic cylinder surface) with the ratio ω between the half major axis, a, and the collector length, L for different values of the aspect ratio λ.

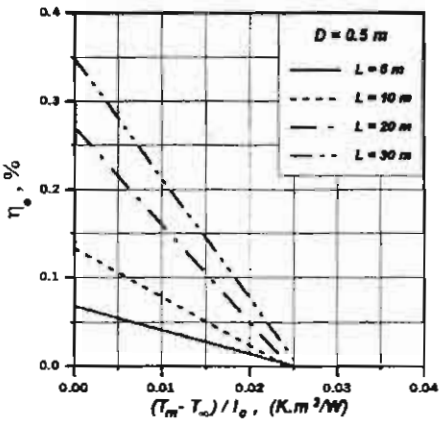

Fig.10: Exergy efficiency as a function of the collector length

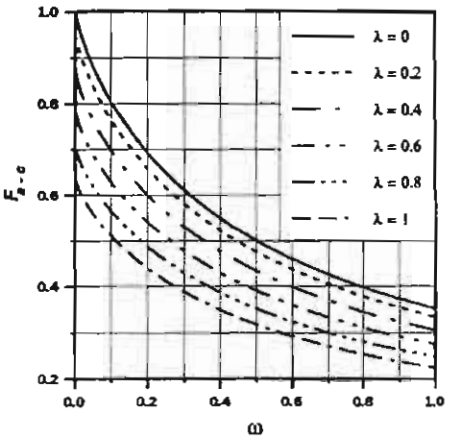

Fig.11: Variation of the shape factor with the ratio a/L

It is clear from the figure that the configuration factor equals unity at no air flow and at infinite length of collector. It decreases with decreasing the collector length or increasing the aspect ratio, i.e. with increasing the air flow rate, until it reaches the full-load condition. The rate of decrease is relatively high for low values of ω and small for high values. The configuration factor approaches zero as ω goes to ∞. The eonfiguration factor at full-loaded collector (circular cylinder surface) is represented versus the collector length and with the diameter as a parameter in Fig.12. It may be noticed that the angle factor decreases with increasing D and increases with increasing L to approach the value $2/\pi$ as L goes to ∞.

Figure 13 shows the estimated variation in solar irradiance on clear days allover the year in Shebin El-Kom, Egypt at latitude 31.25°N with the time of day every hour from 6 to 18 O'clock as a parameter. The calculated solar insolation on the first day of each month along the day is shown in Fig.14 from January to June and in Fig.15 from July to December while the same variation is plotted in Fig.16 but for the first day of the four seasons of the year.

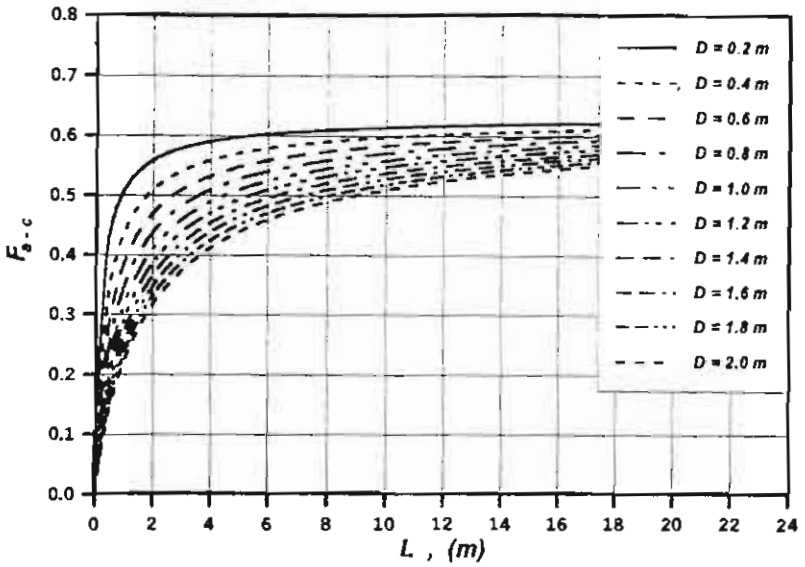

Fig.12: Variation of the configuration factor with both length and diameter of the solar air-heater in case of full-loaded condition

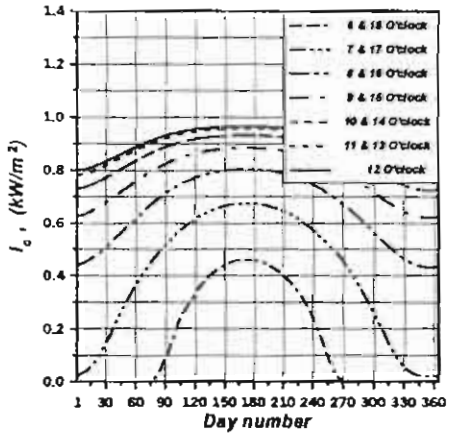

Fig.13: Change of the solar insolation with the day number in Shebin El-Kom every hour of the sun-shine period

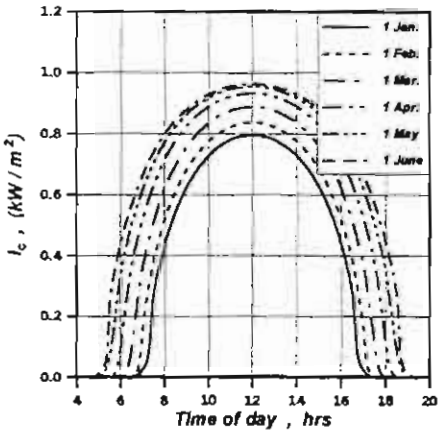

Fig.14: Change of the solar insolation with the time of day in Shebin El-Kom on the first day of month from January to June

The experimental results obtained according to the standard test method of the National Bureau of Standards (NBS), Ref.[21], are plotted in Fig.17. The experimental investigations are carried out on three types of flexible cylindrical solar air-heaters namely, collector 1 with a single cover, collector 2 with double covers and collector 3 with double covers and a back insulation. The results indicate that the solar air-heater having double covers and a back insulation has the highest thermal efficiency while that of a single cover and without a back insulation has the lowest efficiency. The slopes of the data fit lines are nearly the same and equal to 0.036 kW/m^{2}K as a mean value. This slope represents the

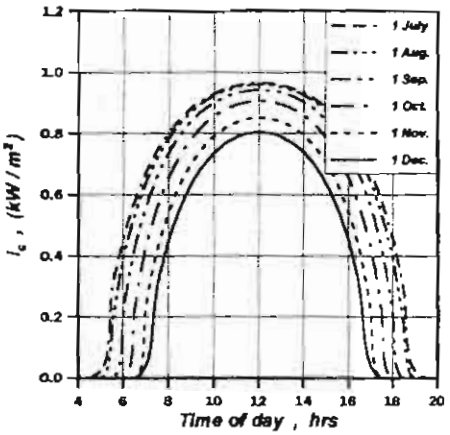

Fig.15: Change of the solar insolation with the time of day in Shebin El-Kom on the first day of month from July to December

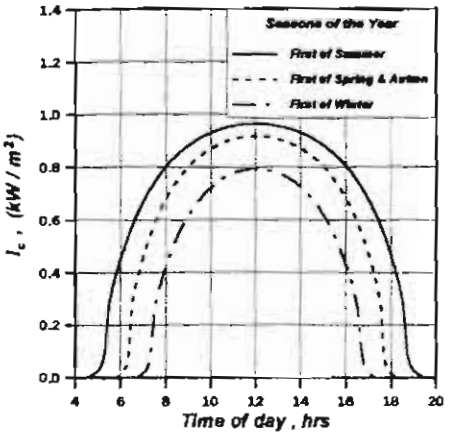

Fig.16: Change of the solar insolation with the time of day in Shebin El-Kom on the first of each season

product of the heat removal factor, F_R, and the overall unit conductance from the collector surface to the ambient air, U_c. Figure 18 gives the percentage increase in the thermal efficiency of collector 2, due to the existence of two covers that decreases the top heat loss, with respect to the thermal efficiency of collector 1, which has a single cover. This percentage increase ranges from 33% to 72% in the calculated range of the appropriate parameter $\Delta T/I_c$. Similarly, the percentage increase in the thermal efficiency of collector 3, which has two covers and a back insulation, relative to collector 1 is also represented in Fig.18. The application of a back insulation, which minimizes the back heat loss, yields an excess increase in the thermal efficiency to reach about 57% to 198% of the thermal efficiency of collector 1, for insolation range from about 200 to 900 W/m^2.

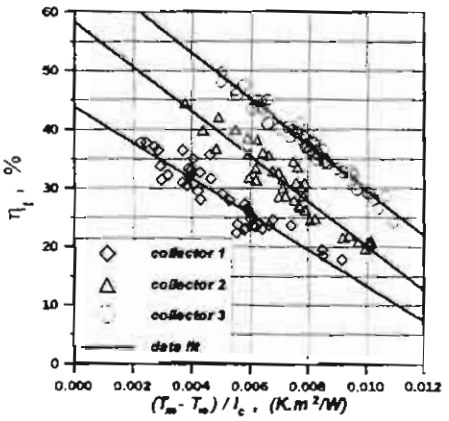

Fig.17: Experimental results of the thermal efficiency of the three tested solar air-heaters

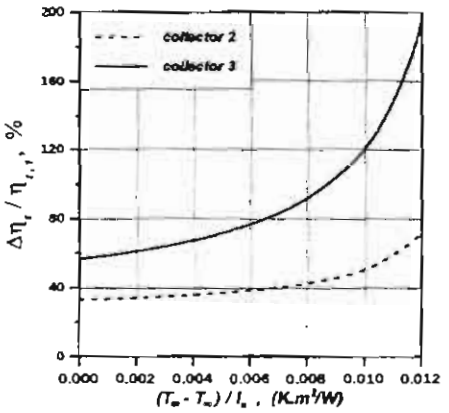

Fig.18: Percentage increase in the thermal efficiency of collectors 2 & 3 with respect to collector 1

A comparison between the experimental results and the theoretical investigations for the thermal efficiency of collector 1 is presented in Fig.19. The comparison shows a good agreement. Another comparison is made in Fig.20 between the experimental and theoretical studies for the collector exergy efficiency. It indicates also a satisfactory agreement. Figure 21 represents a comparison between experimental data and theoretical prediction of the configuration factor between the absorber and the cover of the solar air-heater as a function of the half major axis, a, and the collector length, L. A good agreement is found between both results.

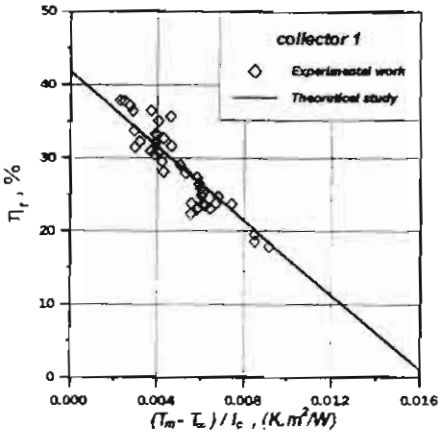

Fig.19: Comparison of the experimental data with the numerical solution for the thermal efficiency

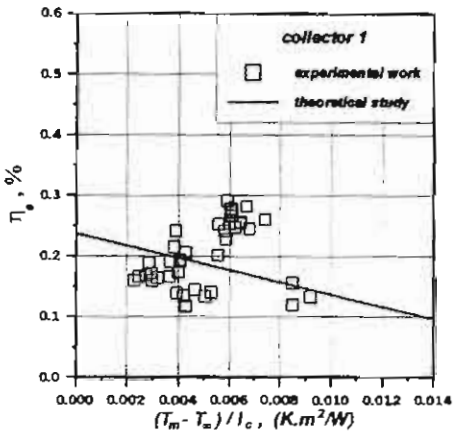

Fig.20: Comparison of the experimental results with the numerical analysis for the exergy efficiency

Inspection of the plotted data in Fig.22 shows that Nu versus Re logarithmic plot is linear. The resulting correlation for Nusselt number between the absorber and the heated air is obtained to be as follows:

$$Nu = 0.156\,\mathrm{Re}^{0.57}.$$

Through comparison of the foregoing developed correlation with the test data, the correlation is found to be fairly representative to the experimental results, as seen from Fig.22. Both the correlation and the test data are compared once more with Malik and Buelow equation [2] for air-heating flat-plate solar collectors with a single plastic cover. This equation takes the following form:

$$Nu = \frac{0.0192\,\mathrm{Re}^{3/4}\,\mathrm{Pr}}{1+1.22\,\mathrm{Re}^{-1.8}(\mathrm{Pr}-2)},$$

with $\mathrm{Pr} = 0.7$ for air and Re is based on the hydraulic diameter. A good agreement is found between the three compared results, as shown in Fig.22.

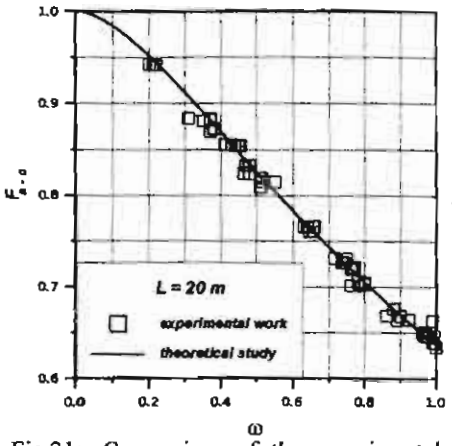

Fig.21: Comparison of the experimental results with the analytical study for the configuration factor

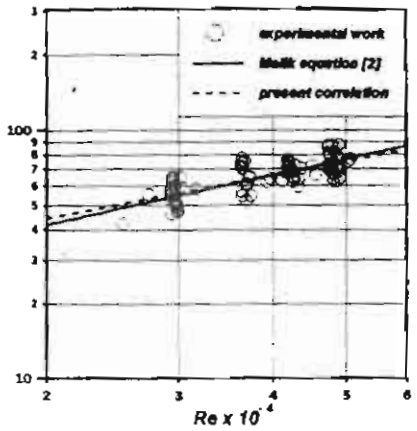

Fig.22: Comparison of the experimental data for Nu with the present correlation and with a published correlation of another author

CONCLUSIONS

The performance of a plastic cylindrical solar air-heater for heating processes is studied theoretically and experimentally, from the standpoint of thermal energy and exergy. As a result, it is shown that the thermal efficiency falls linearly with the appropriate parameter $\Delta T/I_c$. It increases with decreasing the collector diameter and with increasing the collector length. The rate of increase is high for small diameters and short lengths of collector. The thermal efficiency of a cylindrical collector having two covers is more than that of a single cover. This is because the existence of two covers decreases the top heat loss rather than a single cover. The percentage increase ranges from 33% to 72% for $\Delta T/I_c$ lies between 0 and 0.012 K.m^2/W. Moreover, the applying of a back insulation, which minimizes the back heat loss, gives an excess increase in the thermal efficiency to reach about 57% to 198% of the thermal efficiency of the cylindrical solar air-heater having only one cover and without a back insulation. The exergy efficiency of a cylindrical solar air-heater, which expresses the maximum available work obtained from the thermal energy gain, increases with decreasing its diameter or increasing its length. It has much lower values than the thermal efficiency.

The configuration factor equals unity at no air flow and at infinite length of collector. It decreases with decreasing the collector length or increasing the aspect ratio until it reaches the full-loaded condition. In this case, the configuration factor increases with increasing the length to approach the value $2/\pi$ as the length goes to infinity.

A simple correlation for predicting Nusselt number between the absorber and the heated air is developed. The correlation is found to be fairly representative to the experimental data and agrees satisfactorily with a previously published

correlation of another authors. The included comparisons between the numerical, analytical and experimental results show also good agreements.

LITERATURE

[1] Suri, R.K. and Saini, J. S. : "Performance Prediction of Single- and Double-Exposure Solar Air-Heaters" ; Solar Energy, v 12, pp. 525-530, (1969).

[2] Malik, M.A. and Buelow, F.H. : "Heat Transfer in a Solar Heated Air Duct-Simplified Analysis" ; in "Heliotechnique and Development" v 2, pp. 31-37, Development Analysis Associates, Cambridge, Massachusetts, (1976).

[3] Close, D. : "Solar – Air Heaters for Low and Moderate Temperature Applications" ; Solar Energy, v 7, p. 117, (1963).

[4] Gupta, C.L. and Garg, H.P. : "Performance Studies on Solar Air – Heaters" ; Solar Energy, v 11, p. 25, (1967).

[5] Rao, S.K. and Suri, R.K.: "Optimization of Flat-Plate Solar Collector Area"; Solar Energy, v 12, p. 531, (1969).

[6] Kreith, F. and Kreider, J. : "Principles of Solar Engineering" ; Chap. 2 & 4, McGraw-Hill Book Company, (1978).

[7] Al-Kamil, M. and Al-Ghareeb, A.: "Effect of Thermal Radiation Inside Solar Air Heaters" ; Energy Conversion and Management, v 38, n 14, pp. 1451-1458, (1997).

[8] Hachemi, A. : "Thermal Performanee Enhancement by Interaction between the Radiation and Convection in Solar Air Heaters" ; Renewable Energy, v 12, n 4, pp. 419-433, (1997).

[9] Ong, K.: "Thermal Performance of Solar Air Heaters: Mathematical Model and Solution Procedure" ; Solar Energy, v 55, n 2, pp. 93-109, (1995)

[10] Ong, K. : "Thermal Performance of Solar Air Heaters: Experimental Correlation" ; Solar Energy, v 55, n 3, pp. 209-220, (1995).

[11] Choudhury, C., Chauhan, P. and Garg, H.:"Design Curves for Conventional Solar Air Heaters" ; Renewable Energy, v 6, n 7, pp. 739-749, (1995).

[12] Toups, K.A. : "A General Computer Program for the Determination of Radiant-Interchange Configuration and Form Factors" ; CONFAC II, North America Aviation, Inc., Space and Information Systems Division, NASA-4133, (1965).

[13] Hamiliton, D. C. and Morgan, W.R. : "Radiant Interchange Configuration Factors" ; NACA Tech. Note 2836, (1952).

[14] Sparrow, E. M. and Cess, R. D.: "Radiation Heat Transfer" ; McGraw-Hill Book Company, New York, Chap. 4, (1978).

[15] Holman, J. P. : "Heat Transfer" ; Sixth Edition, McGraw-Hill, Book Company, New York, Chap. 8, p. 373, (1963).

[16] Isachenko, V.; Osipova, V. and Sukomel, A. : "Heat Transfer" ; Part 4, Chap. 15, pp. 467-470, Mir Publishers, Moscow, (1969).

[17] Sparrow, E. M. : "A New and Simpler Formulation for Radiative Angle Factors" ; Trans. of the ASME J. of Heat Transfer, pp. 81-88, (1963).

[18] Yuan, S.W. : "Foundations of Fluid Mechanics" ; Prentice-Hall of India Pvt. Ltd., (1969).

[19] McCormick, J.M., and Salvadori, M.G. : "Numerical Methods in Fortran" ; Fourth Edition, Prentice-Hall, New Delhi, Chap.4, pp. 59-68, (1985).

[20] Spiegel, M. R. : "Mathematical Handbook of Formulas and Tables" ; Schaum's Outline Series, McGraw-Hill Book Company, New York, (1970).

[21] Simon, F.F. : "Flat Plate Solar Collector Performance Evaluation with a Solar Simulator as a Basis for Collector Selection and Performance Prediction" ; NASA Rept. TM X-71793, 1975, see also Solar Energy, v 18, pp. 451-466, (1976).